

Functional Coupling of the β_1 Subunit to the Large Conductance Ca^{2+} -activated K^+ Channel in the Absence of Ca^{2+}

Increased Ca^{2+} Sensitivity from a Ca^{2+} -independent Mechanism

Crina M. Nimigean and Karl L. Magleby

From the Department of Physiology and Biophysics, University of Miami School of Medicine, Miami, Florida 33101-6430

abstract Coexpression of the β_1 subunit with the α subunit (*mSlo*) of BK channels increases the apparent Ca^{2+} sensitivity of the channel. This study investigates whether the mechanism underlying the increased Ca^{2+} sensitivity requires Ca^{2+} , by comparing the gating in 0 Ca^{2+}_i of BK channels composed of α subunits to those composed of $\alpha+\beta_1$ subunits. The β_1 subunit increased burst duration ~ 20 -fold and the duration of gaps between bursts ~ 3 -fold, giving an ~ 10 -fold increase in open probability (P_o) in 0 Ca^{2+}_i . The effect of the β_1 subunit on increasing burst duration was little changed over a wide range of P_o achieved by varying either Ca^{2+}_i or depolarization. The effect of the β_1 subunit on increasing the durations of the gaps between bursts in 0 Ca^{2+}_i was preserved over a range of voltage, but was switched off as Ca^{2+}_i was increased into the activation range. The Ca^{2+} -independent, β_1 subunit-induced increase in burst duration accounted for 80% of the leftward shift in the P_o vs. Ca^{2+}_i curve that reflects the increased Ca^{2+} sensitivity induced by the β_1 subunit. The Ca^{2+} -dependent effect of the β_1 subunit on the gaps between bursts accounted for the remaining 20% of the leftward shift. Our observation that the major effects of the β_1 subunit are independent of Ca^{2+}_i suggests that the β_1 subunit mainly alters the energy barriers of Ca^{2+} -independent transitions. The changes in gating induced by the β_1 subunit differ from those induced by depolarization, as increasing P_o by depolarization or by the β_1 subunit gave different gating kinetics. The complex gating kinetics for both α and $\alpha+\beta_1$ channels in 0 Ca^{2+}_i arise from transitions among two to three open and three to five closed states and are inconsistent with Monod-Wyman-Changeux type models, which predict gating among only one open and one closed state in 0 Ca^{2+}_i .

key words: maxi-K channel • K_{Ca} channel • single-channel • mSlo • Monod-Wyman-Changeux

INTRODUCTION

Large conductance Ca^{2+} -activated K^+ channels (BK channels or maxi-K channels)¹ are found in a wide variety of tissues, where they regulate excitability through a negative feedback mechanism (Meech and Standen, 1975; Meech, 1978; Adams and Gage, 1980; Marty, 1981, 1983; Pallotta et al., 1981; Maruyama et al., 1983; Cook, 1984; Blatz and Magleby, 1987; Petersen and Findlay, 1987; Singer and Walsh, 1987; Smart, 1987; Hudspeth and Lewis, 1988; Brayden and Nelson, 1992; Wu et al., 1995; Tanaka et al., 1997; Jones et al., 1999; and reviewed by Hille, 1991; Conley, 1996; Kaczorowski et al., 1996). Both membrane depolarization and increased intracellular Ca^{2+} (Ca^{2+}_i) activate BK channels. Opened

BK channels allow the efflux of K^+ , which then hyperpolarizes the membrane potential, reducing excitability and closing Ca^{2+} channels. BK channels can be composed of either α subunits alone (α channels) or of α subunits together with various β subunits ($\alpha+\beta$ channels). The larger pore-forming α subunits, which are encoded by the gene at the *slo* locus, were first cloned from *Drosophila* (*slowpoke* phenotype), and bear homology to the superfamily of voltage-gated K^+ channels, including a pore-forming region between the S5 and S6 transmembrane segments, and an S4 voltage-sensing domain (Atkinson et al., 1991; Adelman et al., 1992; Salkoff et al., 1992; Butler et al., 1993; Dworetzky et al., 1994; Pallanck and Ganetzky, 1994; Tseng-Crank et al., 1994; Wallner et al., 1995; Jan and Jan, 1997; Stefani et al., 1997; Diaz et al., 1998). BK channels differ from strictly voltage-gated K^+ channels by having a greatly extended COOH terminus that accounts for more than half of the primary sequence. The extended COOH terminus contains at least one Ca^{2+} -binding domain involved in activation of the channel (Wei et al., 1994; Schreiber and Salkoff, 1997; Schreiber et al., 1999).

Several distinct auxiliary β subunits for the BK channel have been cloned: β_1 , β_2 , and β_3 (Knaus et al., 1994; Meera et al., 1996; Dworetzky et al., 1996; Tseng-Crank et

Portions of this work were previously published in abstract form (Nimigean, C.M., and K.L. Magleby. 2000. *Biophys. J.* 78:91A; and Nimigean, C.M., B.L. Moss, and K.L. Magleby. 1999. *Soc. Neurosci. Abstr.* 25:985).

Address correspondence to Crina M. Nimigean or Karl L. Magleby, Department of Physiology and Biophysics, R430, P.O. Box 016430, Miami, FL 33101-6430. Fax: 305-243-6898; E-mail: cnimigea@chroma.med.miami.edu or kmagleby@miami.edu

¹Abbreviations used in this paper: BK channel, large conductance Ca^{2+} -activated K^+ channel; GFP, green fluorescent protein; HEK cells, human embryonic kidney cells; MWC, Monod-Wyman-Changeux.

al., 1996; Oberst et al., 1997; Wallner et al., 1999; Xia et al., 1999). All of these β subunits appear to share a common secondary structure with two transmembrane domains connected by a large, extracellular loop. The different β subunits affect the gating of the α subunits in several ways. The β_1 subunit increases the apparent Ca^{2+} sensitivity by decreasing the Ca^{2+}_i required for half activation of the channel (McManus et al., 1995; Dworetzky et al., 1996; Tseng-Crank et al., 1996; Wallner et al., 1996; Meera et al., 1996; Nimigeon and Magleby, 1999; Ramanathan et al., 2000). The increased Ca^{2+} sensitivity with the β_1 subunit is reflected in a 5–10-fold leftward shift in plots of open probability (P_o) vs. Ca^{2+}_i (Nimigeon and Magleby, 1999). In addition to increasing the Ca^{2+} sensitivity like the β_1 subunit, the β_3 subunit produces an inactivating BK channel similar to the BK channels in chromaffin cells (Wallner et al., 1999; Xia et al., 1999). The action of the β_1 subunit requires an S0 transmembrane segment in BK channels that is not present in other voltage-gated K^+ channels (Wallner et al., 1996; Meera et al., 1997).

In a recent study, we showed that the β_1 subunit increases the apparent Ca^{2+} sensitivity of BK channels by stabilizing the channel in the bursting states (Nimigeon and Magleby, 1999). The β_1 subunit increased P_o by increasing burst duration ~ 20 -fold while having little effect on the durations of the gaps between bursts in the presence of Ca^{2+}_i . Increasing P_o by either adding the β_1 subunit or by increasing Ca^{2+}_i gave marked differences in the single-channel kinetics, suggesting that the β_1 subunit does not increase P_o by proportionally increasing all the Ca^{2+} -binding rates. These observations of differences in gating kinetics induced by Ca^{2+}_i and the β_1 subunit raise the possibility that the β_1 subunit may not require Ca^{2+}_i to exert its facilitating effects on P_o .

We now investigate this possibility by examining the effects of the β_1 subunit on the gating of unliganded BK channels, by studying the gating of α and $\alpha+\beta_1$ channels in the virtual absence of Ca^{2+}_i . Such experiments are possible since BK channels can gate in effective 0 Ca^{2+}_i (Pallotta, 1985; Meera et al., 1996; Horrigan et al., 1999; Horrigan and Aldrich, 1999; Talukder and Aldrich, 2000). We find, in the absence as well as the presence of Ca^{2+}_i , that the β_1 subunit has the same effect of retaining the gating of the channel in the bursting states. Hence, neither Ca^{2+} -dependent transitions nor Ca^{2+} binding are required for the β_1 subunit-induced prolongation of bursts, and, consequently, for the functional coupling of the β_1 subunit to the channel. Therefore, the increase in Ca^{2+} sensitivity that arises from the β_1 subunit-induced increase in burst duration arises mainly from a Ca^{2+} -independent mechanism. The effects of the β_1 subunit on stabilizing the bursting states were observed over a range of membrane potentials (+30 to +100 mV). Increasing P_o with either the β_1 subunit or by depolarization gave marked differences

in the single-channel kinetics, suggesting that the β_1 subunit does not increase P_o by the same alterations in rate constants that voltage induces.

Previous studies (Meera et al., 1996) have indicated that physiological Ca^{2+}_i acts as a switch to functionally couple the β_1 subunits with the α subunits, thus allowing lower levels of Ca^{2+}_i to activate the BK channel by shifting the P_o vs. Ca^{2+}_i curve to the left. We examined the mechanism of this switch and found that the observation that the β_1 subunit increases mean burst duration ~ 20 -fold, independent of Ca^{2+}_i , is sufficient to account for 80% of the increase in Ca^{2+} sensitivity indicated by the leftward shift in the P_o vs. Ca^{2+}_i curve. The remaining 20% of the leftward shift arises because the β_1 subunit no longer increases (and may decrease slightly) the durations of gaps between bursts in the presence of Ca^{2+}_i . Thus, the functional switch has both Ca^{2+} -independent and -dependent components, with the Ca^{2+} -independent component accounting for the majority of the increase in Ca^{2+} sensitivity. While the effect of the β_1 subunit on increasing burst duration is always present, independent of Ca^{2+}_i , it is only in the presence of Ca^{2+}_i , when the P_o becomes significant, that this β_1 subunit-induced increase in burst duration has a physiological effect. For example, increasing P_o 20-fold, from 0.0002 to 0.004 in very low Ca^{2+}_i , would have little effect on current, whereas increasing P_o 20-fold, from 0.02 to 0.40 in higher Ca^{2+}_i , could have a dramatic physiological effect.

The complex bursting kinetics in 0 Ca^{2+}_i for both α and $\alpha+\beta_1$ channels was found to arise from transitions among a minimum of two to three open states and three to five closed states. Gating among such a large number of unliganded states is inconsistent with gating mechanisms based on Monod-Wyman-Changeux type models for ligand-activated tetrameric allosteric proteins (Monod et al., 1965), which would predict gating among only one open and one closed state in 0 Ca^{2+}_i (Horrigan et al., 1999; Talukder and Aldrich, 2000). Gating among multiple open and closed states in 0 Ca^{2+}_i is consistent with a 50-state two-tiered gating mechanism proposed by Rothberg and Magleby (1999) for the gating of BK channels.

METHODS

Heterologous Expression of BK Channels in Human Embryonic Kidney 293 Cells

Human embryonic kidney (HEK) 293 cells were transiently transfected with expression vectors (pcDNA3) encoding the α subunit (*mSlo* from mouse; Genbank accession number MMU09383) and β_1 subunit (bovine β ; Genbank accession number L26101) of the BK channels kindly provided by Merck Research Laboratories, and also with an expression vector encoding the green fluorescent protein (GFP, Plasmid pGreen Lantern-1; GIBCO BRL). Cells were transfected transiently using the Lipofectamine Reagent (Life Technologies) according to the protocol provided by GIBCO BRL. The GFP was used to monitor successfully transfected cells. HEK

cells are optimal for transfection and expression after they have been in culture for ~3–4 wk. The cells are cultured using standard tissue culture media: DMEM with 5% fetal bovine serum (Life Technologies) and 1% penicillin-streptomycin solution (Sigma-Aldrich) and passaged at ~100% confluency using PBS with 5 mM EDTA to loosen cells from the bottom of the dish. For transfection, cells at 30–40% confluency in 30-mm Falcon dishes used later for recording were first washed with antibiotic and serum-free DMEM, and then incubated with a mixture of the plasmids (total of 1 μ g DNA per dish), Lipofectamine Reagent (optimal results at 7 μ l) and Opti-MEM I reduced serum medium (Life Technologies). The mixture was left on cells for 1–1.5 h, after which it was replaced with standard tissue culture media. The culture media was again replaced after 24 h to remove debris and dead cells. The cells were patch-clamped 2–3 d after transfection when the culture medium was replaced with standard extracellular saline solution that contained (mM) 2.04 CaCl₂, 2.68 KCl, 1.48 MgCl₂, 0.05 MgSO₄, 125 NaCl, 0.83 NaH₂PO₄, 20 NaHCO₃, and 2 HEPES, pH 7.4.

In the coexpression experiments, a fourfold molar excess of plasmid encoding the β_1 subunit was used to drive coassembly with the α subunits (McManus et al., 1995). Using the same promoter (cytomegalovirus) for the α and β_1 subunits and the GFP increased the probability that if the GFP was expressed, the included subunits would also be expressed.

Solutions

The intracellular solution contained 175 mM KCl, 5 mM TES pH buffer, and 10 mM EGTA and 10 mM HEDTA to buffer the Ca²⁺ (see below). The extracellular solution contained either 150 or 175 mM KCl and 5 mM TES and had no added Ca²⁺ or Ca²⁺ buffers. Both the intracellular and extracellular solutions were adjusted to pH 7.0. The amount of Ca²⁺ added to the intracellular solution to obtain approximate free Ca²⁺ concentrations of 0.001–100 μ M was calculated using stability constants for EGTA (Smith and Miller, 1985) and for HEDTA (Martell and Smith, 1993). The 0 Ca²⁺ solution had no Ca²⁺ added and the same composition as the other solutions. These solutions were then calibrated using a Ca²⁺ electrode (Ionplus; Orion Research, Inc.) standardized against solutions with KCl and TES in which known amounts of Ca²⁺ were added. Before adding Ca²⁺, any contaminating divalent cations were removed from the solution by treatment with Chelex 100 (Bio-Rad Laboratories). The solutions bathing the intracellular side of the patch were changed by means of a valve-controlled, gravity-fed perfusion system using a micro-chamber (Barrett et al., 1982).

Single-Channel Recording and Analysis

Currents flowing through single (or in some cases multiple) BK channels in patches of surface membrane excised from HEK 293 cells transfected with clones for either the α or the α and β_1 subunits were recorded using the patch-clamp technique (Hamill et al., 1981). All recordings were made using the excised inside-out configuration in which the intracellular surface of the patch was exposed to the bathing solution. BK channels were identified by their large conductance and characteristic voltage and Ca²⁺ dependence (Barrett et al., 1982). Endogenous BK channels in non-transfected HEK 293 cells were not seen, but we cannot exclude that they might exist at a low density. Currents were recorded with an Axopatch 200A amplifier and stored on VCR tapes using a VR-10B digital data recorder. The currents were then analyzed using custom programs written in the laboratory. Single-channel patches were identified by observing openings to only a single open-channel conductance level during prolonged recording in which the

open probability was >0.4. Experiments were performed at room temperature (20–25°C). For the 0-Ca²⁺_i experiments, the number of channels in a patch was determined by pulling the patch in a high Ca²⁺ solution and then switching to 0 Ca²⁺ solution.

Single-channel current records were low-pass filtered with a four-pole Bessel filter to give a final effective filtering (–3 dB) of typically 10 kHz (range 4.5–10 kHz), and were sampled by computer at a rate of 125–250 kHz. The methods used to select the level of filtering to exclude false events that could arise from noise, measure interval durations with half-amplitude threshold analysis, and use stability plots to test for stability and identify modes have been described previously, including the precautions taken to prevent artifacts in the analysis (McManus et al., 1987; McManus and Magleby, 1988, 1989; Magleby, 1992). The kinetic analysis in this study was restricted to channel activity in the normal mode, which typically involves 96% of the detected intervals (McManus and Magleby, 1988). Activity in modes other than normal, including the low activity mode (Rothberg et al., 1996), was removed before analysis, as were the infrequent transitions to subconductance levels. The numbers of intervals during normal activity analyzed for each experimental condition ranged from 50 to 14,000 in the 0-Ca²⁺_i experiments, where the open probability and the interval frequency can be very low at less depolarized potentials, to upwards of 200,000 for higher Ca²⁺_i, where the channel activity was higher.

Data from multichannel patches were only analyzed for very low Ca²⁺_i, where the activity was so low that simultaneous openings of two or more channels were seldom if ever observed. For the multichannel patches, the open probability was calculated by dividing the total open time by the total record length, and then by the number of channels in the patch. The mean durations of the gaps between bursts for the multichannel patches were estimated by determining these parameters as if the data were from a single channel, and then multiplying the estimates by the numbers of channels in the patch. The mean closed times for the multichannel patches were determined in the following way: the sum of all durations of the gaps between the bursts during the total recording time, multiplied by the number of channels in the patch, was added to the sum of all the durations of the closed intervals within bursts, and then the value was divided by the total number of closed intervals in the record. There was no need to correct estimates of the mean open time and mean number of openings per burst, since at such low P_o , only one channel was open at any given time.

The methods used to log-bin the intervals into dwell-time distributions, fit the distributions with sums of exponential components using maximum likelihood fitting techniques (intervals less than two dead times were excluded from the fitting), and determine the number of significant exponential components with the likelihood ratio test have been described previously (McManus and Magleby, 1988, 1991; Colquhoun and Sigworth, 1995). Dwell-time distributions are plotted with the Sigworth and Sine (1987) transformation, which plots the square root of the number of intervals per bin without correcting for the logarithmic increase in bin width with time. With this transform, the peaks of the individual components fall at the time constants of the components.

The method of defining a critical gap (closed interval) to identify bursts is detailed in Magleby and Pallotta (1983). In brief, the distributions of closed-interval durations were first typically fitted with the sum of five exponential components. The closed intervals from the one or two exponential components with the longest time constants were then defined as gaps between bursts, as there was typically a difference of one to three orders of magnitude in the time constants separating the gaps between bursts from the time constants of the much briefer duration components that generated the closed intervals within bursts. A critical time was then defined so that the number of gap intervals misclas-

sified as closed intervals within bursts was equal to the number of closed intervals within bursts misclassified as gap intervals. With this critical time, errors resulting from misclassification would tend to cancel out. The critical time was found to be relatively insensitive to the numbers of significant exponentials required to fit the dwell-time distribution. Burst analysis was typically restricted to current records from single channels, except for some multi-channel patches where P_o was so low (due to low Ca^{2+}_i and/or less positive voltages) that only one channel was open at any time. Burst analysis was restricted to data with $P_o < 0.8$, as it was difficult to clearly define the gaps between bursts for higher P_o .

RESULTS

The β_1 Subunit Increases both P_o and Burst Duration in the Virtual Absence of Ca^{2+}_i

To investigate whether the β_1 subunit requires Ca^{2+}_i for its action, we used single-channel analysis to examine the gating of α and $\alpha+\beta_1$ channels in the effective absence of Ca^{2+}_i (<1 nM), which will be referred to as 0 Ca^{2+}_i . (It will be shown in a later section that effective 0 Ca^{2+}_i was achieved.) Fig. 1 A shows single-channel currents recorded in 0 Ca^{2+}_i at +30 mV from an α channel and also from an $\alpha+\beta_1$ channel. The occasional openings and bursts of openings are separated by the long closed intervals of many seconds that form the gaps between bursts. The long gaps between bursts in 0 Ca^{2+}_i give very low open probability. The average P_o s for the entire records from which each excerpt was obtained were 0.00056 for the α channel and 0.0039 for the $\alpha+\beta_1$ channel, for a sevenfold increase in P_o . The mean P_o for 15 α channels and 21 $\alpha+\beta_1$ channels at 0 Ca^{2+}_i is plotted in Fig. 2 A (left-

most points), where the presence of the β_1 subunit increased $P_o \sim 10$ -fold on average, from ~ 0.0002 to 0.002.

In conjunction with the large increase in P_o , the β_1 subunit stabilized the bursting states, increasing mean burst duration in 0 Ca^{2+}_i . For the channels in Fig. 1, mean burst duration increased from 1.1 to 28.8 ms, for a 26-fold increase. The dramatic increase in mean burst duration can be seen in Fig. 1 B, where selected bursts are presented on a faster time base. The β_1 subunit consistently increased burst duration in 0 Ca^{2+}_i . Mean burst duration for 15 α channels and 21 $\alpha+\beta_1$ channels at 0 Ca^{2+}_i is plotted in Fig. 2 C (left-most points). The presence of the β_1 subunit increased mean burst duration 21-fold in 0 Ca^{2+}_i , from 0.59 to 12.4 ms. Thus, the β_1 subunit exerts its characteristic effects of increasing P_o by retaining the gating in the bursting states in 0 Ca^{2+}_i , just as it does in the presence of Ca^{2+}_i . For comparison, the effects of the β_1 subunit on gating in the presence of Ca^{2+}_i (1.8 μ M) are shown in Fig. 1 C, where the β_1 subunit also increased burst duration and P_o , as described previously (Nimigeen and Magleby, 1999).

The β_1 Subunit Alters the Gating Parameters from 0 to Higher Ca^{2+}_i

To examine further the effects of the β_1 subunit on the gating at 0 Ca^{2+}_i and to compare these effects with those at higher Ca^{2+}_i , we measured an array of kinetic parameters (P_o , mean burst duration, mean duration of gaps between bursts, mean open time, mean closed time, and mean number of openings per burst) for α

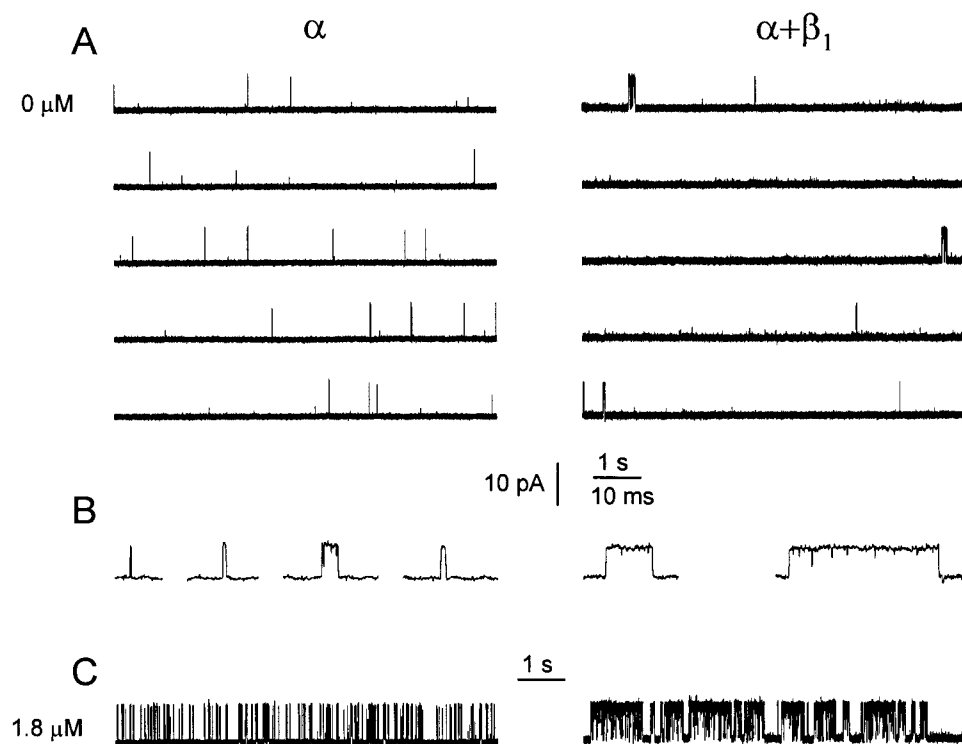


Figure 1. The β_1 subunit alters the single-channel gating kinetics in both the absence and presence of Ca^{2+}_i . (A) Currents recorded from single α and $\alpha+\beta_1$ channels in 0 Ca^{2+}_i . A continuous record in each case was cut into the five presented traces. The β_1 subunit increases both burst duration and the duration of the gaps between bursts. The average P_o s for the entire record from which each excerpt was obtained were: 0.00056 for the α channel and 0.0039 for the $\alpha+\beta_1$ channel. (B) Bursts from α and $\alpha+\beta_1$ channels presented on a faster time base. (C) Currents recorded from α and $\alpha+\beta_1$ channels in 1.8 μ M Ca^{2+}_i . The traces were filtered at 4 kHz for display in this and subsequent figures, while the filtering for the analysis carried out in this paper was typically 10 kHz. Membrane potential: +30 mV; α channel, C92; $\alpha+\beta_1$ channel, C87.

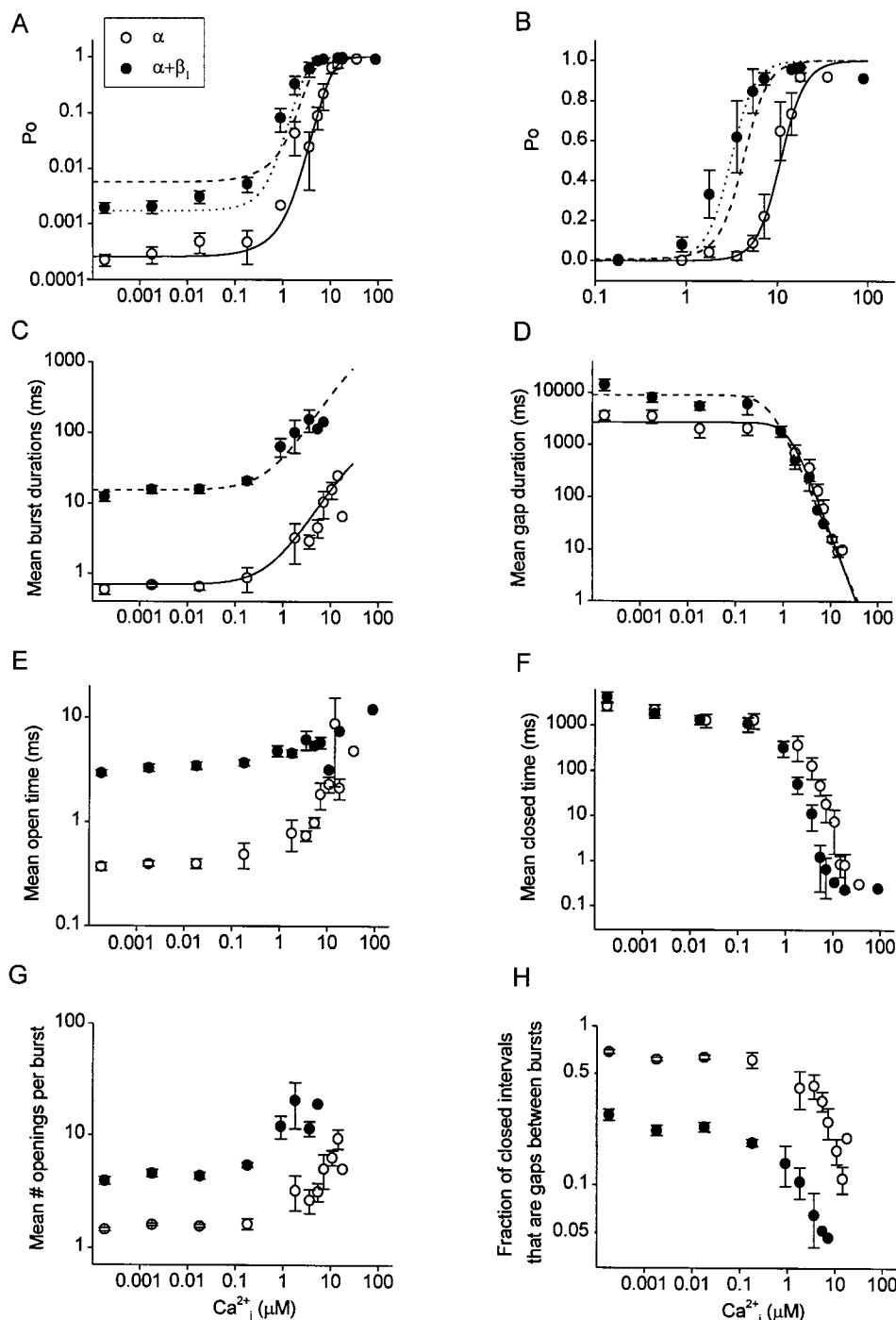


Figure 2. Effects of the β_1 subunit on the gating parameters from 0 to high levels of Ca^{2+}_i . Data is plotted for α channels (\circ) and $\alpha+\beta_1$ channels (\bullet). The lack of effect of Ca^{2+}_i on the parameters from 0.00018 to 0.018 μM Ca^{2+}_i indicates that effective 0 Ca^{2+}_i was achieved in this range. (A and B) Plots of P_o vs. Ca^{2+}_i on double logarithmic and semilogarithmic coordinates. (Continuous lines) Calculated P_o for α channels with Eq. 2 using the continuous line in C for burst and the continuous line in D for gaps. (Dashed lines) Calculated P_o for $\alpha+\beta_1$ channels with Eq. 2 using the dashed line in C for burst and the continuous line in D for gap. The assumption that the β_1 subunit increased burst duration 22-fold in a Ca^{2+} -independent manner accounted for 80% of the leftward shift in the P_o vs. Ca^{2+}_i plot. (Dotted lines) Calculated P_o for $\alpha+\beta_1$ channels with Eq. 2 using the dashed line in C for burst and the dashed line in D for gap. 100% of the shift could be accounted for by also including the smaller Ca^{2+} -dependent effect of the β_1 subunit on the duration of the gaps between bursts. (C) Plot of mean burst duration versus Ca^{2+}_i . The burst duration of α channels (continuous line) was described by the empirical expression: $Y_\alpha(\text{burst}) = 0.7 + 100/[1 + (50/X)^{1.1}]$, where X is Ca^{2+}_i in micromolar and burst duration is in milliseconds. Multiplying this line by a constant factor of 22 then described the burst duration of $\alpha+\beta_1$ channels (dashed line). (D) Plot of the mean duration of gaps between bursts versus Ca^{2+}_i . The continuous line for α channels is given by the empirical equation: $Y_\alpha(\text{gap}) = 2,700\{1 - 1/[1 + (1.3/X)^{2.4}]\}$, and the dashed line for $\alpha+\beta_1$ channels is given by: $Y_{\alpha+\beta}(\text{gap}) = 9,000\{1 - 1/[1 + (0.5/X)^{2.1}]\}$, where X is Ca^{2+}_i in micromolar and gap

duration is in milliseconds. (E–H) Plots of the indicated parameters versus Ca^{2+}_i . For all parts of the figure, the data for α channels are from 15 patches containing 1–12 channels per patch, and the data for $\alpha+\beta_1$ channels are from 21 patches containing 1–13 channels per patch. Data from multichannel patches were used only in 0 or very low Ca^{2+}_i , when the P_o was sufficiently low that the bursts did not overlap. Parameters from multichannel patches were corrected for the numbers of channels in each patch, as specified in methods. Data are plotted as the mean \pm SEM.

and $\alpha+\beta_1$ channels and plotted them against Ca^{2+}_i in Fig. 2. Over the entire range of Ca^{2+}_i , from 0 to higher levels, the β_1 subunit increased mean burst duration ~ 20 -fold (Fig. 2 C). This increase in the mean burst duration arose from both an increase in mean open time

(Fig. 2 E) and in the mean number of openings per burst (Fig. 2 G). The β_1 subunit also increased the mean durations of the gaps between bursts approximately threefold in 0 Ca^{2+}_i , while having little effect on the durations of the gaps at higher Ca^{2+}_i (Fig. 2 D).

The mean closed time was little affected by the β_1 subunit in 0 Ca^{2+}_i (Fig. 2 F) because the β_1 subunit-induced increase in the duration of the gaps between bursts (Fig. 2 D) was compensated for by a decrease in the fraction of closed intervals that were gaps between bursts (Fig. 2 H).

Evidence for the Effective Absence of Ca^{2+}

In Fig. 2 it can be seen that all the measured kinetic parameters (P_o , mean burst duration, mean duration of gaps between bursts, mean open time, mean closed time, and mean number of openings per burst) remained relatively unchanged as Ca^{2+}_i was increased more than two orders of magnitude (from 0.00018 to 0.018 μM). If Ca^{2+}_i were to bind to the channel and affect activity over this wide range of Ca^{2+}_i , then the kinetic parameters that define gating should change. Since little change was observed, these observations suggest that the channel remained functionally unliganded for $\text{Ca}^{2+}_i < 0.1 \mu\text{M}$. Hence, even though trace Ca^{2+}_i was likely present, functional 0 Ca^{2+}_i was achieved.

The β_1 Subunit Shifts the P_o vs. Ca^{2+}_i Curve to the Left

The characteristic leftward shift in the P_o vs. Ca^{2+}_i curve induced by the β_1 subunit (Nimigeau and Magleby, 1999; Ramanathan et al., 2000; and equivalent findings in McManus et al., 1995; Dworetzky et al., 1996; Meera et al., 1996; Tseng-Crank et al., 1996; Wallner et al., 1996) is shown in Fig. 2 B. This leftward shift is generally referred to as an increase in Ca^{2+} sensitivity because it indicates that less Ca^{2+}_i is required to half-acti-

vate the channel. From the semilogarithmic plot in Fig. 2 B, it appears that the β_1 subunit only alters gating for $\text{Ca}^{2+}_i > 0.1 \mu\text{M}$. Hence, this figure by itself suggests that the mechanism involved in the leftward shift in P_o by the β_1 subunit may be a function of Ca^{2+}_i . However, from the double logarithmic plots in Fig. 2, C, E, G, and H, it appears that a major effect of the β_1 subunit is to shift the kinetic parameters associated with burst duration, independent of Ca^{2+}_i . The resulting effect of the β_1 subunit on P_o is shown on double logarithmic coordinates in Fig. 2 A, where P_o is shifted upward both in the absence and presence of Ca^{2+}_i .

β_1 Subunit Exerts Its Effects Over a Range of Voltages

The data in Fig. 2 were obtained at a single voltage of +30 mV. To examine whether the effects of the β_1 subunit in 0 Ca^{2+}_i are dependent on voltage, we collected data in 0 Ca^{2+}_i over a range of voltages. Examples of single-channel currents obtained at +60 and +90 mV for α and $\alpha+\beta_1$ channels are shown in Fig. 3. The β_1 subunit increased the durations of the bursts as well as the gaps between bursts at both voltages. The increase in burst duration with the β_1 subunit in 0 Ca^{2+}_i is clearly shown in Fig. 3 C for both voltages, where representative bursts are presented on a faster time base.

The mean effects of the β_1 subunit on the gating kinetics over a range of voltages in 0 Ca^{2+}_i are shown in Fig. 4 for eight patches with α channels and nine patches with $\alpha+\beta_1$ channels. For both α and $\alpha+\beta_1$ channels, depolarization increased P_o through increases in mean burst duration, mean open time, and the mean

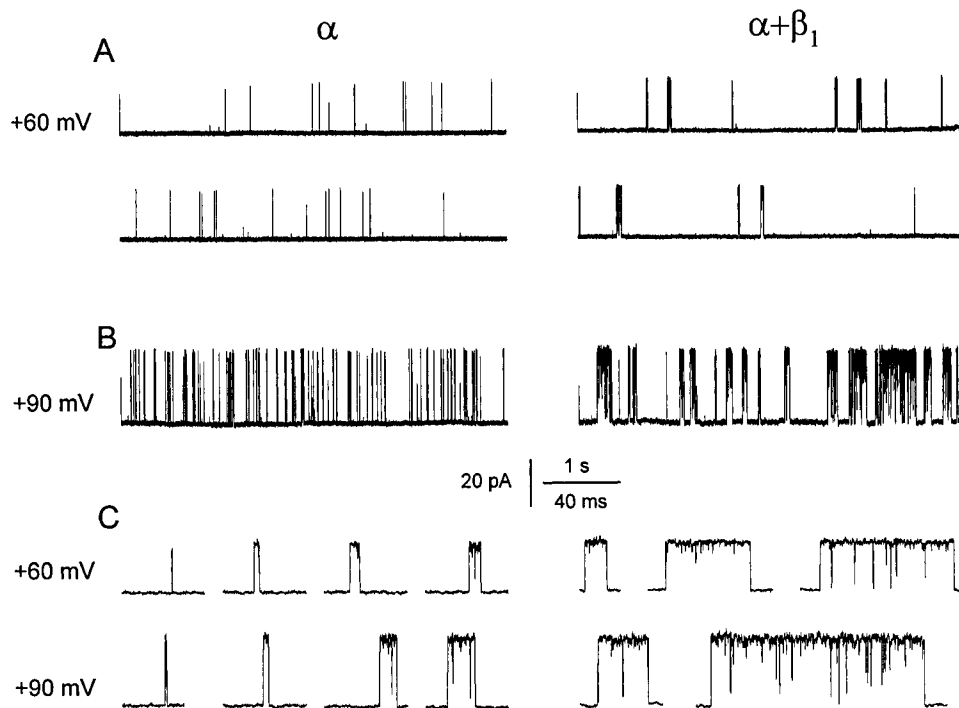


Figure 3. The β_1 subunit still increases both burst duration and the duration of gaps between bursts in 0 Ca^{2+}_i when P_o is increased by depolarization. (A and B) Currents recorded from single α and $\alpha+\beta_1$ channels at two different membrane potentials of +60 mV (A) and +90 mV (B) in 0 Ca^{2+}_i . For the +60-mV data, a continuous record was cut into two traces in each case. The average P_o s for the entire records from which the excerpts were obtained were: 0.0042 (+60 mV) and 0.063 (+90 mV) for the α channel, and 0.029 (+60 mV) and 0.37 (+90 mV) for the $\alpha+\beta_1$ channel. (C) Representative bursts of openings from A and B on a faster time base. α channel, C96; $\alpha+\beta_1$ channel, C100.

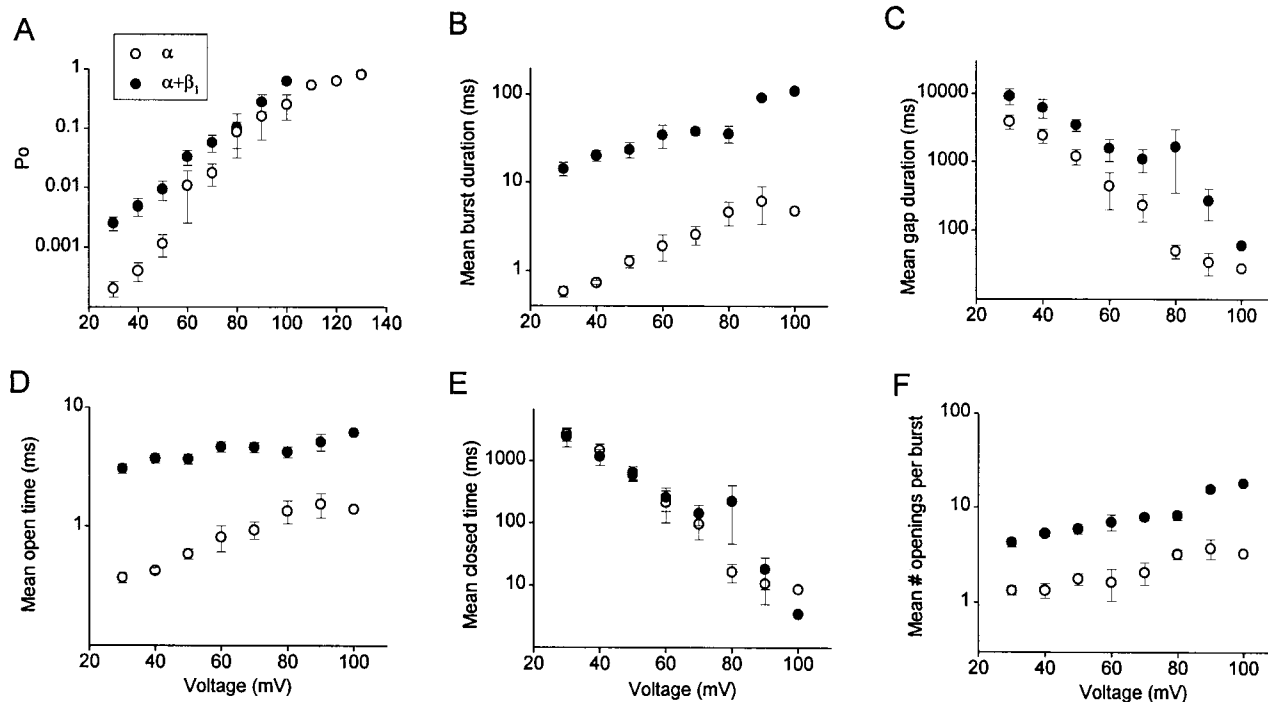


Figure 4. The β_1 subunit exerts its characteristic effects on gating in 0 Ca^{2+}_i from +30 to +100 mV. Data are plotted for α channels (\circ) and $\alpha+\beta_1$ channels (\bullet). All data were obtained in 0 Ca^{2+}_i . (A–F) Plots of the indicated kinetic parameters versus membrane potential. The β_1 subunit increased P_o (A), mean burst duration (B), the mean duration of gaps between bursts (C), mean open time (D), and the mean numbers of openings per bursts (F) over the examined range of membrane potentials by shifting the parameters on the double logarithmic plots, while having little effect on the mean closed times (E). The data for α channels are from eight patches containing 1–12 channels and the data for $\alpha+\beta_1$ channels are from nine patches containing 1–13 channels. Multichannel patches were used only when the P_o was sufficiently low that bursts did not overlap. Parameters from multichannel patches were corrected for the number of channels in each patch. Data are plotted as the mean \pm SEM.

number of openings per burst, and decreases in the mean closed time and in the mean duration of the gaps between bursts (Fig. 4). The same characteristic effects of the β_1 subunit that were observed in 0 Ca^{2+}_i in Fig. 2 were then superimposed on these effects of depolarization. Over the examined range of voltage (+30 to +100 mV), the β_1 subunit increased mean burst duration ~ 20 -fold (Fig. 4 B) and the mean duration of the gaps between bursts two- to threefold (Fig. 4 C). The increase in mean burst duration was due to increases in both mean open time (approximately eightfold, Fig. 4 D), and the mean number of openings per burst (approximately threefold, Fig. 4 F). The β_1 subunit had little effect on mean closed time even though the mean closed time drastically decreased with depolarization (Fig. 4 E).

Evident in Fig. 4 is that the estimates of the parameters that describe single-channel kinetics for α and $\alpha+\beta_1$ channels (mean open time, mean closed time, mean burst duration, mean duration of gaps between bursts, and mean number of openings per burst) are generally parallel with each other on a logarithmic scale, indicating that the ratios of the kinetic parameters for the $\alpha+\beta_1$ to the α channels remain relatively

constant over the examined range of +30 to +100 mV. As a first approximation, a constant ratio suggests that the β_1 subunit may act like a gain control, independent of voltage, such that the kinetic parameters measured in the presence of the β_1 subunit are simply the result of multiplication between the kinetic parameters in the absence of the β_1 subunit and a constant factor, which depends on the parameter measured.

Interestingly, the magnitude of the fractional increase in P_o with the β_1 subunit decreased with depolarization (Fig. 4 A). Some decrease with depolarization might be expected since depolarization increases P_o and P_o saturates near 0.96 for both α and $\alpha+\beta_1$ channels. However, the decreased effect of the β_1 subunit on P_o with depolarization was apparent at low P_o s as well. Projection of imaginary lines through the data in Fig. 4 A suggests that at very depolarized voltages, the β_1 subunit may no longer have an effect of increasing P_o and may even decrease it. A similar trend, however slight, is also apparent in Fig. 4, B and D, for mean burst duration and mean open time, suggesting that the β_1 subunit may have reduced effects on these parameters at greatly depolarized voltages.

The β_1 Subunit Does Not Act Like an Increase in Membrane Potential

Previous results (Nimigean and Magleby, 1999) indicated that the β_1 subunit does not act like an increase in Ca^{2+}_i . That is, the β_1 subunit does not increase all the Ca^{2+} -binding rates proportionally. This conclusion was reached by showing that α and $\alpha + \beta_1$ channels had markedly different gating kinetics at the same P_o , achieved by changing Ca^{2+}_i . We now apply the same type of analysis to investigate whether the β_1 subunit acts like an increase in voltage.

If voltage and the β_1 subunit worked through the same mechanism, α and $\alpha + \beta_1$ channels should display identical gating kinetics at the same P_o , achieved by changing voltage. This was not the case. Increasing P_o with the β_1 subunit in 0 Ca^{2+}_i was associated with greatly increased burst duration and a smaller increase in the duration of the gaps between bursts. In contrast,

increasing P_o with depolarization was associated with small increases in burst duration and large decreases in the duration of gaps between bursts.

Although these differential effects on kinetics are apparent from the examination of Figs. 1–4, they are more easily seen in Fig. 5, where the P_o of an α channel was increased with depolarization to match the P_o of an $\alpha + \beta_1$ channel. The dramatic differences in single-channel kinetics at similar P_o s for α and $\alpha + \beta_1$ channels are readily apparent in the current traces inset in Fig. 5. These effects of voltage and the β_1 subunit on kinetics are quantified in Fig. 5 by the open dwell-time distributions (left) and the closed dwell-time distributions (right) for both the α and the $\alpha + \beta_1$ channels. At similar P_o s, both the mean open times and the mean durations of the gaps between bursts were about an order of magnitude less for the α channel than for the $\alpha + \beta_1$ channel (vertical lines), while the relative number of closed intervals that were

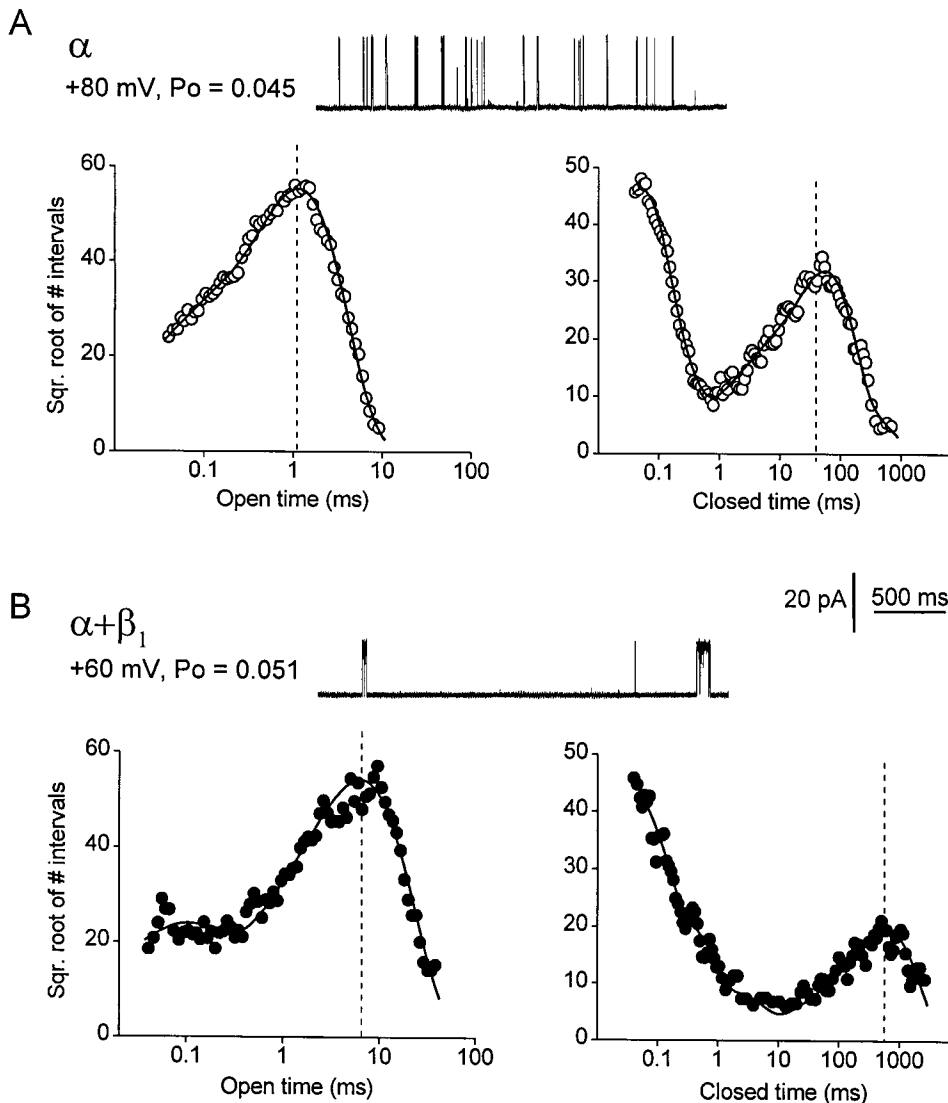


Figure 5. Dwell-time distributions obtained from single α and $\alpha + \beta_1$ channels, adjusted to have the same P_o by changing the voltage, have different single-channel kinetics. The open- and closed-interval durations were log binned, and the square root of the number of intervals in each bin was plotted against the bin midtimes for one α channel (+80 mV) and one $\alpha + \beta_1$ channel (+60 mV) in 0 Ca^{2+}_i . To allow direct comparison of the distributions, the number of intervals in each distribution (from time 0 to infinity) was normalized to 100,000 in each case. The continuous lines are fits with the sums of two significant open and five significant closed exponential components for the α channel and two significant open and four significant closed exponential components for the $\alpha + \beta_1$ channel. The vertical dashed lines indicate the mean open times and the mean durations of the gaps between bursts. The time constants and areas of the exponential components are: (A, open) 0.075 ms, 0.10; 1.1 ms, 0.90. (B, open) 0.081 ms, 0.14; 6.3 ms, 0.86. (A, closed) 0.046 ms, 0.55; 0.13 ms, 0.11; 4.5 ms, 0.033; 54 ms, 0.29; 211 ms, 0.016. (B, closed) 0.041 ms, 0.66; 0.24 ms, 0.17; 1.8 ms, 0.027; 607 ms, 0.14. α channel, C96; $\alpha + \beta_1$ channel, C98.

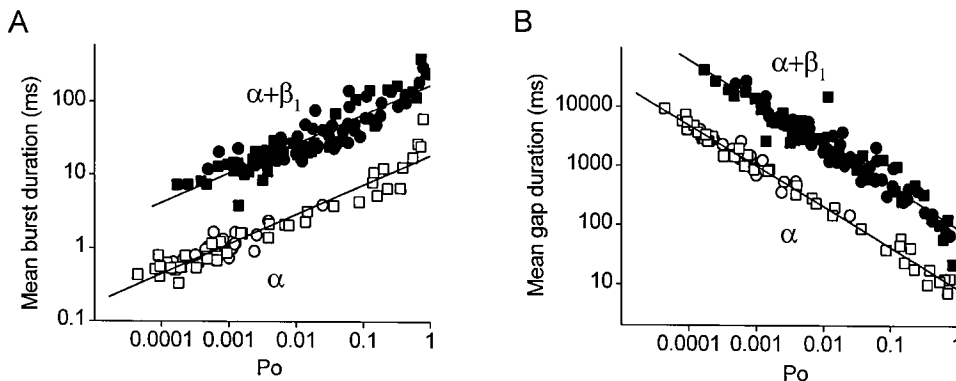


Figure 6. The β_1 subunit-induced increase in both burst and gap duration is independent of P_o and whether the channel is activated by voltage or Ca. (A) Plot of mean burst duration versus P_o . (B) Plot of the mean durations of gaps between bursts versus P_o . Data in each plot are presented for α channels (open symbols) and for $\alpha+\beta_1$ channels (filled symbols). P_o was changed by changing Ca^{2+}_i at the same membrane potential of +30 mV (circles), or by changing the membrane potential in the absence of Ca^{2+}_i (squares). Data are from the same patches detailed in the legends of Figs. 2 and 4.

gaps between bursts was greater for the α channel than for the $\alpha+\beta_1$ channel. These marked differences in the kinetics of α and $\alpha+\beta_1$ channels at the same P_o (achieved by changing voltage) suggest that depolarization and the β_1 subunit act through different mechanisms.

The β_1 Subunit Acts as a Gain Control on Bursting Kinetics, Independent of whether the Channel Is Activated by Voltage or Ca^{2+}_i

To explore whether the β_1 subunit has the same effect on the bursting kinetics, independent of whether P_o is changed by voltage or Ca^{2+}_i , mean burst duration and the mean duration of gaps between bursts were plotted against P_o for both α and $\alpha+\beta_1$ channels in Fig. 6. The circles plot data obtained over a range of Ca^{2+}_i (0 to 18 μ M) at +30 mV, and the squares plot data obtained over a range of voltages (+30 to +100 mV) in 0 Ca^{2+}_i . Filled symbols plot data from $\alpha+\beta_1$ channels and open symbols plot data from α channels. At any given P_o , both the mean burst duration and the mean duration of gaps between bursts were 10-fold longer in the $\alpha+\beta_1$ channels as compared with the α channels, independent of whether the P_o was achieved by changing Ca^{2+}_i or voltage. This 10-fold effect of the β_1 subunit on the bursting parameters was independent of P_o , as indicated by the parallel shifts over four orders of magnitude of change in P_o .

The results in Fig. 6 suggest that the β_1 subunit acts mainly as a gain control on the bursting parameters, independent of P_o or whether the channel is activated by Ca^{2+}_i or by voltage. This is the case since a parallel shift on a logarithmic coordinate, as in Figs. 2, 4, and 6, is consistent with a multiplicative (gain) effect. Hence, as a first approximation, the gain effect of the β_1 subunit appears to be independent of Ca^{2+}_i (Fig. 2), voltage (Fig. 4), and P_o , over the examined range of conditions.

The constant shift in the mean durations of gaps between bursts in Fig. 6 B in the presence of the β_1 subunit

may appear paradoxical, since it was observed in Fig. 2 D that the β_1 subunit increased the durations of the gaps between bursts approximately threefold in 0 Ca^{2+}_i , but had little effect on the durations of the gaps once Ca^{2+}_i was increased. The difference between Figs. 6 and 2 is that the data in Fig. 6 are plotted against P_o rather than Ca^{2+}_i . At a fixed Ca^{2+}_i , the β_1 subunit greatly increased burst duration, leading to an increase in P_o for $\alpha+\beta_1$ channels. The same P_o could then be achieved in α channels by increasing their activity through depolarization or increased Ca^{2+}_i . This increased activity is associated with large decreases in the durations of the gaps between bursts and smaller increases in burst duration (Figs. 2 and 4). Hence, at the same P_o , α channels must have much smaller gaps between bursts than $\alpha+\beta_1$ channels, as observed (Fig. 6 B), to compensate for the much longer duration bursts of $\alpha+\beta_1$ channels (Fig. 6 A).

Ca^{2+}_i Switches Off the β_1 Subunit-induced Increase in the Duration of Gaps between Bursts

As indicated previously, for 0 Ca^{2+}_i , the β_1 subunit increased the durations of gaps between bursts approximately threefold (Fig. 2 D). For $Ca^{2+}_i > \sim 0.2 \mu$ M, the β_1 subunit no longer lengthened the durations of the gaps between bursts (perhaps even decreased them slightly), consistent with Nimigean and Magleby (1999). Thus, Ca^{2+}_i switches off (inhibits) the β_1 subunit-induced lengthening of the gaps between bursts. It follows that the Ca^{2+} -dependent effect of the β_1 subunit on the mean closed time in Fig. 2 F is a consequence of $Ca^{2+}_i > 0.2 \mu$ M switching off the β_1 subunit-induced lengthening of bursts. Thus, although the major effects of the β_1 subunit on increasing burst duration appear to be independent of Ca^{2+}_i , the observation of a Ca^{2+} -dependent effect on the durations of the gaps between bursts raises the question as to what extent the β_1 subunit-induced shift in apparent Ca^{2+} sensitivity is Ca^{2+} dependent.

80% of the β_1 Subunit-induced Increase in Ca^{2+} Sensitivity Is Independent of Ca^{2+}_i

To determine to what extent the β_1 subunit-induced shift in Ca^{2+} sensitivity is Ca^{2+} independent, we examined how much of the β_1 subunit-induced shift in Ca^{2+} sensitivity could be accounted for by assuming that the sole effect of the β_1 subunit was to multiply burst duration a constant amount, independent of Ca^{2+}_i . We first developed an empirical model to generate the P_o vs. Ca^{2+}_i data for α channels, and then calculated the predicted P_o vs. Ca^{2+}_i curve for $\alpha + \beta_1$ channels by assuming that the only effect of the β_1 subunit was to multiply burst duration a constant amount, independent of Ca^{2+}_i .

Open probability is defined by Eq. 1:

$$P_o = \frac{\text{mean open time}}{(\text{mean open time} + \text{mean closed time})}. \quad (1)$$

Since the durations of the closed intervals within bursts are brief compared with both the durations of the open intervals and the durations of the gaps between bursts, P_o can be approximated by:

$$P_o \cong \text{burst} / (\text{burst} + \text{gap}), \quad (2)$$

where burst represents the mean burst duration and gap represents the mean duration of gaps between bursts.

The continuous lines in Fig. 2, C and D, are empirical descriptions of mean burst duration and the mean duration of gaps between bursts, respectively, as functions of Ca^{2+}_i for α channels (see figure legends). These empirical descriptions for burst and gap were then used with Eq. 2 to calculate the P_o vs. Ca^{2+}_i curve for the α channels, plotted as continuous lines in Fig. 2, A and B. It can be seen that this method of predicting P_o gave a reasonable description of the P_o vs. Ca^{2+}_i data for the α channels for both semilogarithmic and double logarithmic plots.

To determine to what extent the increased Ca^{2+} sensitivity induced by the β_1 subunit could be predicted by assuming that the sole effect of the β_1 subunit was to increase burst duration a constant (multiplicative) amount, independent of Ca^{2+}_i , the P_o vs. Ca^{2+}_i curve for $\alpha + \beta_1$ channels was calculated exactly as it was for the α channels, except that mean burst duration (burst) in Eq. 2 was multiplied by a constant factor 22. The results of the calculation (Fig. 2, A–C, dashed lines) show a leftward shift in the P_o vs. Ca^{2+}_i curve that accounts for 80% of the increase in Ca^{2+} sensitivity induced by the β_1 subunit. This simple multiplicative effect also described the effect of the β_1 subunit on burst duration (Fig. 2 C, dashed line). Thus, the assumption that the sole effect of the β_1 subunit was to increase mean burst duration a constant multiplicative amount, independent of Ca^{2+}_i , could describe the β_1 subunit-induced in-

crease in burst duration and 80% of the leftward shift in the P_o vs. Ca^{2+}_i curve induced by the β_1 subunit. It follows, then, that 80% of the β_1 subunit-induced increase in Ca^{2+} sensitivity (the apparent Ca^{2+} switch) can be accounted for by a Ca^{2+} -independent mechanism.

The remaining 20% of the β_1 subunit-induced increase in Ca^{2+} sensitivity did appear to be Ca^{2+} dependent. When the Ca^{2+} -dependent effect of the β_1 subunit on the gaps between bursts was taken into account by describing gap in Eq. 2 with the dashed line in Fig. 2 D (rather than by the continuous line), 100% of the β_1 subunit-induced leftward shift in the Ca^{2+} sensitivity could be accounted for, as shown by the dotted line in Fig. 2, A and B. Furthermore, when the Ca^{2+} -dependent component was included, the P_o in 0 Ca^{2+}_i was also correctly predicted (Fig. 2 A, dotted line). (Results essentially indistinguishable from those presented in this section were obtained when the calculations included the effects of the durations of the intervals within bursts.)

We cannot exclude that there may be Ca^{2+} -dependent effects of the β_1 subunit on mean open time and on the mean number of openings per burst (Fig. 2, E and G). Unfortunately, estimates of these two parameters, unlike burst duration, are highly dependent on the flickers (brief closed intervals within bursts). Since flickers may arise from closed states beyond the activation pathway (Cox et al., 1997; Rothberg and Magleby, 1998, 1999; Talukder and Aldrich, 2000), it is not clear whether there is a Ca^{2+} dependence of the underlying process. Nevertheless, the results of this section indicate that 80% of the β_1 subunit-induced increase in Ca^{2+} sensitivity arises from a Ca^{2+} -independent increase in burst duration and 20% arises from a Ca^{2+} -dependent inhibition of the lengthening effect of the β_1 subunit on the gaps between bursts at +30 mV.

Unliganded BK Channels Gate in a Minimum of Two to Three Open and Three to Five Closed States

To obtain further insight into the gating mechanism of unliganded α and $\alpha + \beta_1$ channels, an estimate of the number of kinetic states entered during gating in 0 Ca^{2+}_i for each channel were obtained by fitting dwell-time distributions of open- and closed-interval durations with sums of exponential components. The number of significant exponential components gives a measure of the minimal number of kinetic states entered during gating (Colquhoun and Hawkes, 1981, 1982, 1995; McManus and Magleby, 1988). Examples of such dwell-time distributions obtained in 0 Ca^{2+}_i are shown in Fig. 5, where the open distributions were described by two significant open components for both α and $\alpha + \beta_1$ channels and the closed distributions were described by five significant closed components for α channels and four significant closed components for $\alpha + \beta_1$ channels. Estimates from eight patches contain-

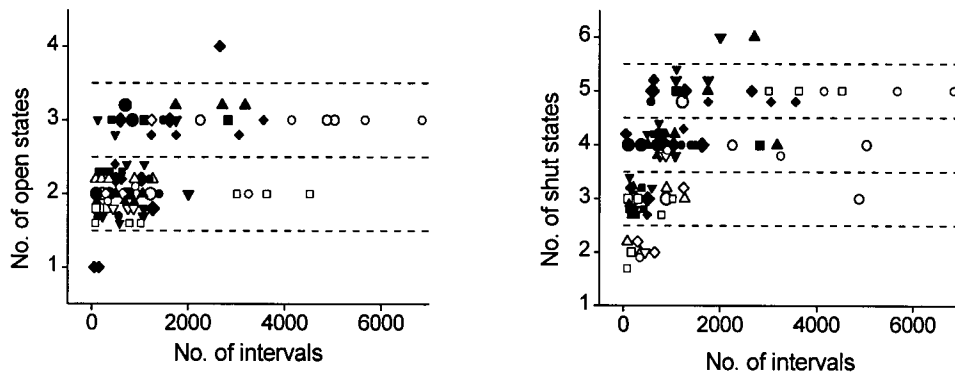


Figure 7. BK channels typically gate in a minimum of two to three open and three to five closed states in 0 Ca^{2+}_i , inconsistent with gating mechanisms based on the Monod-Wyman-Changeux model with Ca^{2+}_i as the allosteric activator, which predicts gating in one open and one closed state in 0 Ca^{2+}_i . The minimal number of significant exponential components required to describe the open and closed dwell-time distributions in 0 Ca^{2+}_i are plotted against the numbers

of analyzed intervals. Data for α channels (open symbols) are from 34 sets of data from eight different patches. Data for $\alpha+\beta_1$ channels (filled symbols) are from 52 sets of data from 12 patches. A number of data sets, each at a different membrane potential, were typically obtained from each patch. Each symbol type plots estimates obtained from a single patch. Data from patches containing multiple channels were included when the channel activity was so low that channel openings did not occur simultaneously. When the analysis was restricted to the 27 data sets from the seven patches containing a single channel, the same results were obtained, except that only two, rather than three, open states were detected for α channels. There was no obvious effect of voltage on the number of detected states.

ing α channels and 12 patches containing $\alpha+\beta_1$ channels are presented in Fig. 7 for data obtained over a range of voltages in 0 Ca^{2+}_i .

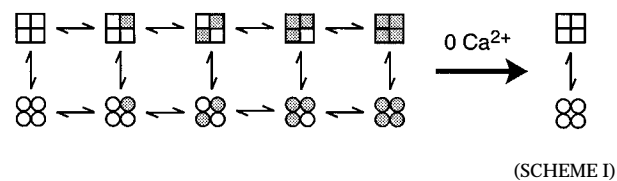
Both α and $\alpha+\beta_1$ channels typically gated in a minimum of two to three open states and three to five closed states in 0 Ca^{2+}_i . (Similar results were found when analysis was restricted to the 27 data sets from the seven patches containing a single channel.) These estimates can be compared with a minimum of typically three to four open and five to six closed states for α and $\alpha+\beta_1$ at higher levels of activity in the presence Ca^{2+}_i (Nimigeon and Magleby, 1999), and to typically three to four open and five to seven closed states for native BK channels from cultured rat skeletal muscle in the presence of Ca^{2+}_i (McManus and Magleby, 1988). The larger numbers of detected states at higher Ca^{2+}_i when compared with 0 Ca^{2+}_i may reflect in part the increased resolution resulting from the increased numbers of intervals (see McManus and Magleby, 1988) that could be collected and analyzed in higher Ca^{2+}_i , where the activity was greatly increased.

In 0 Ca^{2+}_i , the estimates of the mean number of detected open states for α channels (2.2 ± 0.4 , mean \pm SD) was not significantly different ($P > 0.25$, Mann-Whitney test) from the mean number of detected open states for the $\alpha+\beta_1$ channels (2.4 ± 0.6). The estimate of the mean number of detected closed states for α channels (3.4 ± 1.0) was significantly less ($P < 0.05$) than the number of detected closed states entered for $\alpha+\beta_1$ channels (4.1 ± 0.8). An increased number of detected closed states for $\alpha+\beta_1$ channels in 0 Ca^{2+}_i could reflect a difference in the actual numbers of states typically entered during gating in 0 Ca^{2+}_i , or an increased ability to detect closed states for $\alpha+\beta_1$ channels because the intervals are spread over a greater range of times than for α channels.

Our findings of gating among multiple open and closed states in 0 Ca^{2+}_i are consistent with a study using single-channel recording just published by Talukder and Aldrich (2000), where data were presented for gating in two to three open and three closed states in 0 Ca^{2+}_i for *mslo* channels composed of only the α subunit. The fewer closed states detected in their study may reflect that fewer closed states were typically entered at the more depolarized voltages used in their study or that the detection of closed states was more difficult because of the compressed dwell time distributions at the higher P_o s in their study.

Rejection of the Monod-Wyman-Changeux Model for Gating in 0 Ca

Models considered for the gating of BK channels have often been based on the Monod-Wyman-Changeux (MWC) model for allosteric proteins (McManus and Magleby, 1991; DiChiara and Reinhart, 1995; Wu et al., 1995; Cox et al., 1997; Cui et al., 1997; Rothberg and Magleby, 1998). The MWC model (Monod et al., 1965) is presented in Scheme I, where the upper row represents closed states, the lower row represents open states, and shaded subunits have bound Ca^{2+}_i .



The opening-closing transitions in the MWC model are concerted, with all four subunits undergoing simultaneous conformational changes. From Scheme I, it

can be seen that the gating will be confined to the two unliganded states in the absence of Ca^{2+}_i , giving only one open and one closed state. The observations in Fig. 7, that both α and $\alpha+\beta_1$ channels typically gate in a minimum of two to three open and three to five closed states in 0 Ca^{2+}_i are clearly at odds with Scheme I, and require that the MWC model be rejected as a mechanism for the gating of these channels. Talukder and Aldrich (2000) have also rejected the MWC model for gating of BK channels based on the observation of gating in multiple open and closed states in 0 Ca^{2+}_i . Findings using other types of experimental approaches have previously shown that the gating of BK channels is inconsistent with the MWC model (Scheme I) or extensions of the MWC model (Horrigan et al., 1999; Horrigan and Aldrich, 1999; Rothberg and Magleby, 1998, 1999).

DISCUSSION

The accessory β_1 subunit of BK channels greatly increases their Ca^{2+} sensitivity by reducing the Ca^{2+}_i required for half activation 5–10-fold, giving a characteristic leftward shift in the P_o vs. Ca^{2+}_i plots (McManus et al., 1995; Dworetzky et al., 1996; Meera et al., 1996; Tseng-Crank et al., 1996; Wallner et al., 1996; Nimigean and Magleby, 1999; Ramanathan et al., 2000; and Fig. 2 B). Although it is known that the β_1 subunit increases P_o in the presence of Ca^{2+}_i by retaining the gating in the bursting states (Nimigean and Magleby, 1999), the method of coupling between the α and β_1 subunits is not yet established. One possibility is that the functional coupling between α and β_1 subunits requires Ca^{2+}_i (Meera et al., 1996). To test this, we examined the effects of the β_1 subunit on the gating in the virtual absence of Ca^{2+}_i for comparison to its effects when Ca^{2+}_i is present. In both the absence and presence of Ca^{2+}_i , the β_1 subunit increased burst duration ~ 20 -fold, by increasing both mean open time and the mean number of openings per burst (Fig. 2). The β_1 subunit-induced increase in burst duration increased P_o in both the absence and presence of Ca^{2+}_i (Fig. 2, A and B). Since the β_1 subunit still imposed its dominant effects on channel gating in the absence of Ca^{2+}_i when the channel was unliganded, it follows that neither Ca^{2+} binding nor Ca^{2+} -dependent steps are required for the dominant action of the β_1 subunit.

If the dominant action of the β_1 subunit does not require Ca^{2+} -dependent processes, then the paradoxical possibility arises that the mechanism underlying the β_1 subunit-induced increase in Ca^{2+} sensitivity also does not require Ca^{2+}_i . To explore this possibility, we examined to what extent an assumption of Ca^{2+} -independent action could account for the leftward shift that gave rise to the increased Ca^{2+} sensitivity. We found that 80% of the leftward shift could be accounted for by as-

suming that the only effect of the β_1 subunit was to increase burst duration ~ 20 -fold, independent of Ca^{2+}_i (Fig. 2, A and C, dashed lines). Thus, a Ca^{2+} -independent mechanism was sufficient to account for 80% of the increased Ca^{2+} sensitivity induced by the β_1 subunit.

The remaining 20% of the shift in Ca^{2+} sensitivity reflects a Ca^{2+} -dependent mechanism. The β_1 subunit increased the durations of the gaps between bursts approximately threefold in the absence of Ca^{2+}_i , and this increase disappeared (and the gap durations became slightly briefer based on the fitted lines) as Ca^{2+}_i was raised sufficiently to just increase channel activity (Fig. 2 D). When this Ca^{2+} -dependent effect of the β_1 subunit on gaps between bursts was taken into account, the remaining 20% of the leftward shift in Ca^{2+} sensitivity could be accounted for (Fig. 2, A and B, dotted lines).

Whatever the mechanism for the Ca^{2+} dependence of the β_1 subunit on the durations of gaps between bursts at the transition between 0 and low Ca^{2+}_i , it seems unlikely to reflect a β_1 subunit-induced increase in Ca^{2+}_i binding rates, as the β_1 subunit then had little effect on the durations of the gaps between bursts for further increases in Ca^{2+}_i that decreased the durations of gaps between bursts two orders of magnitude (Fig. 2 D). This relative lack of effect of the β_1 subunit on the gaps between bursts in the presence of Ca^{2+}_i has been described previously (Nimigean and Magleby, 1999) and suggests that the β_1 subunit does not alter the Ca^{2+} -dependent transitions that dominate the gaps between bursts in the presence of Ca^{2+}_i . Since gaps between bursts are present both in the absence and presence of Ca^{2+}_i , their durations are determined by both Ca^{2+} -independent and -dependent transitions. Consequently, a large increase in the rate constants for the Ca^{2+} -dependent transitions as Ca^{2+}_i is increased could mask the effects of the β_1 subunit on the Ca^{2+} -independent transitions involved in lengthening the gaps between bursts in 0 Ca^{2+}_i , without directly affecting such transitions.

Our finding that the β_1 subunit was always functionally coupled to the α subunit, independent of Ca^{2+}_i (Figs. 1–4), differs from that of Meera et al. (1996), who suggest that the functional coupling is exquisitely modulated by Ca^{2+} , with Ca^{2+} ions switching the $\alpha+\beta_1$ complex into a functionally coupled state. This difference in conclusions could arise from a number of factors. First, our experiments used single-channel recording, which allowed high resolution analysis at very low P_o s, while their experiments used macro currents, where activity at low P_o would be more difficult to study. Using single-channel recording, we observed a 10-fold increase in P_o in 0 Ca^{2+}_i in the presence of the β_1 subunit (from 0.0002 to 0.002 at +30 mV), while they reported no change in P_o under similar 0 Ca^{2+}_i . Second, we directly measured the effects of the β_1 subunit on the gating in 0 Ca^{2+}_i , while they estimated the effects

from the projected voltages required for half activation ($V_{0.5}$) in 0 Ca^{2+}_i . Third, our experiments used bovine β_1 and mouse α subunits, while theirs used human β_1 and α subunits. The difference in primary structure of the β_1 subunits (84% homology) and α subunits (96% homology) in the two studies might lead to different mechanisms of modulation by the β_1 subunit.

The contributions of these three factors to the differences in conclusions are not clear, but the most likely explanation is that the β_1 subunit has pronounced effects on P_o in 0 Ca^{2+}_i at moderate depolarized potentials, as we observed, while having little effect on P_o at large depolarizations, as used by Meera et al. (1996) to determine $V_{0.5}$ in 0 Ca^{2+}_i . Such an explanation requires that the effect of the β_1 subunit on increasing P_o be weakly voltage dependent, with depolarization decreasing the magnitude of the effect. Support for this possibility comes from the voltage-dependent trend in our data in P_o , mean burst duration, and mean open time (Fig. 4, A, B, and D). Projections of our data suggest that the effects of the β_1 subunit on P_o may become negligible at large depolarized potentials, and may even reverse. Further support for this possibility comes from observations of Ramanathan et al. (2000) that the β_1 subunit has little effect on estimates of $V_{0.5}$ in low Ca^{2+}_i , and observations of Cox, D.H., and R.W. Aldrich (personal communication) that the effect of the β_1 subunit on increasing conductance in macropatches becomes negligible at subnanomolar Ca^{2+}_i as the potential approaches +150 mV, after which the β_1 subunit decreases the conductance at potentials greater than +150 mV.

We did find that the β_1 subunit had a Ca^{2+} -dependent component, but this component accounted for only 20% of the increased Ca^{2+} sensitivity, and arose mainly from a Ca^{2+} -dependent switching off of the β_1 subunit-induced lengthening of the gaps between bursts (Fig. 2 D). Consistent with our observations of functional coupling in 0 Ca^{2+}_i , Meera et al. (1996) found that the β_1 subunit slowed the activation kinetics threefold in 0 Ca^{2+}_i , just as might be expected from the threefold increase in the duration of gaps between bursts that we observed with the β_1 subunit in 0 Ca^{2+}_i . Other studies have also reported a β_1 -induced slowing in activation and deactivation kinetics over a range of Ca^{2+}_i (Dworetzky et al., 1996; Tseng-Crank et al., 1996; Ramanathan et al., 2000).

If the β_1 subunit is always coupled, then it should be possible to predict the effects of the β_1 subunit on the kinetic parameters in the absence of Ca^{2+}_i by projecting data obtained in the presence of Ca^{2+}_i to the abscissa at 0 Ca^{2+}_i . Such projections are difficult on the log-log plots used in this paper to emphasize the kinetics at low Ca^{2+}_i , because a value of 0 Ca^{2+}_i is never reached on a log axis. However, such projections can be made from the semilogarithmic plots presented in

our previous study. For example, the predicted value of burst duration for $\alpha+\beta_1$ and α channels obtained by projecting a linear regression line to 0 Ca^{2+}_i from the data obtained from 15 to 1.8 μM Ca^{2+}_i was 16 and 0.7 ms, respectively (Nimigeon and Magleby, 1999; Fig. 4 E). These values are in agreement with the limiting values of mean burst duration of 15 and 0.7 ms observed in the present study as Ca^{2+}_i approached 0 (Fig. 2 C, dashed and continuous lines). Thus, the 23-fold increase in burst duration determined by projection is in agreement with the 21-fold increase in burst duration determined by the limiting values in 0 Ca^{2+}_i . Similar agreement in projected and limiting results for the effect of the β_1 subunit was obtained for mean open time and the mean number of openings per burst.

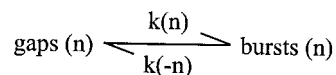
The direct observations in Figs. 1 and 2, and the projected observations discussed above, indicate that the β_1 subunit exerts its characteristic effects of increasing P_o and mean burst duration through an increase in the mean open time and the number of openings per burst in Ca^{2+}_i so low that the channel is essentially unliganded. Consequently, since the β_1 subunit imposes its characteristic effects on channel gating in the absence of Ca^{2+}_i , it follows that the β_1 subunit is coupled to the channel in the absence of Ca^{2+}_i , and can generate its signature effects without changing any Ca^{2+} -binding rates. Furthermore, the observation on the double logarithmic plots in Fig. 2 A that both the α and $\alpha+\beta_1$ channels appear to have similar critical Ca^{2+}_i for initiating the Ca^{2+} -dependent activation (between 0.18 and 0.9 μM Ca^{2+}_i) indicates that the β_1 subunit may have relatively little effect on the initial Ca^{2+} -binding rates, for if it had a pronounced effect, the Ca^{2+} -induced increase in P_o (and underlying changes in the other gating parameters) should occur at appreciably lower Ca^{2+}_i for $\alpha+\beta_1$ channels than for α channels. Cox and Aldrich (2000) have also suggested that the β_1 subunit has little effect on the affinity of the channel's Ca^{2+} -binding sites.

Consistent with a lack of increase in Ca^{2+} -dependent rate constants, observations in our previous study indicate that the β_1 subunit does not act by mimicking the effects of increased Ca^{2+}_i (Nimigeon and Magleby, 1999). Similar kinetic analysis in this present study showed that the β_1 subunit does not act by mimicking the effects of voltage, as increasing P_o with depolarization gave markedly different single-channel gating kinetics than increasing P_o with the β_1 subunit (Fig. 5). This finding, together with the observation that the voltage dependence of the single channel kinetic parameters is little affected by the β_1 subunit (Fig. 4), suggests that the β_1 subunit does not exert its major effects on gating over the examined range of voltages by changing the apparent voltage sensitivity of the channel. This conclusion is in agreement with previous studies that found little difference in the voltage sensitivity between α and

$\alpha + \beta_1$ channels (McManus et al., 1995; Dworetzky et al., 1996; Meera et al., 1996; Tseng-Crank et al., 1996).

The observations in this present study indicate that the major effect of the β_1 subunit is to produce approximately parallel shifts (on logarithmic coordinates) in the magnitudes of the examined bursting parameters, when compared with α channels (Figs. 2 and 4). Such parallel shifts on logarithmic coordinates are consistent with a multiplicative (gain) effect of the β_1 subunit on the examined parameters, and this gain effect was observed over three orders of magnitude of P_o , independent of whether the channel was activated by Ca^{2+}_i or by voltage (Fig. 6). How might such a gain effect on the bursting parameters occur?

The gating of BK channels is described by a model comprised of five parallel subschemes, each with five open and five closed states, in which the subschemes differ from one another by having either 0, 1, 2, 3, or 4 Ca^{2+}_i bound to the states in each subscheme (Rothberg and Magleby, 1999). Recent data obtained for the gating of α channels in 0 Ca^{2+}_i by Horrigan et al. (1999), Horrigan and Aldrich (1999), and Talukder and Aldrich (2000) are also consistent with this two-tiered model. For discussion purposes, this complex gating mechanism can be reduced to the simplified Scheme II, where gaps (n) represent the collection of closed states that generate the gaps between bursts, bursts (n) represent the collection of open and closed states that generate the bursts, $k(n)$ is the forward rate constant for transitions from gaps to bursts, $k(-n)$ is the backward rate constant for leaving bursts, and n, with values of 0, 1, 2, 3 and 4, represents the number of Ca^{2+}_i bound to the states. Note that the rate constants $k(n)$ and $k(-n)$ are composite rate constants that reflect all of the rate constants involved in generating gaps and bursts: $k(n)$ also includes the rate constants among the collection of closed states that generate the gaps, and $k(-n)$ also includes the rate constants among the collection of open and closed states that generate the bursts.



(SCHEME II)

In 0 Ca^{2+}_i , none of the states involved in gating would have bound Ca^{2+} . Binding Ca^{2+} would then increase P_o by altering the rate constants to decrease the durations of gaps and to increase the durations of bursts, and this would be the case for both α and $\alpha + \beta_1$ channels (Fig. 2).

Since the β_1 subunit had little effect on the minimal number of kinetic states entered during gating in 0 Ca^{2+}_i (Fig. 7) or in the presence of Ca^{2+}_i (Nimigeon and Magleby, 1999), the most parsimonious mode of action of the β_1 subunit would be to modulate gating through changes in one or more of the transition rates among

the existing states. Which transitions are altered? The ~ 20 -fold increase in burst duration, independent of Ca^{2+}_i (Fig. 2 C), suggests that the β_1 subunit slows the rate constant $k(-n)$ of ~ 20 -fold, and this would be the case independent of the number of bound Ca^{2+}_i , where $n = 0-4$. Such a slowing would act to retain the gating in the bursting states, increasing P_o . An explanation for the apparent multiplicative (gain) effect of the β_1 subunit now becomes apparent. Whatever the burst duration (which increases with Ca^{2+}_i), the β_1 subunit increases burst duration another ~ 20 -fold by slowing $k(-n)$ ~ 20 -fold, independent of bound Ca^{2+}_i .

Whereas the β_1 subunit increases burst duration ~ 20 -fold, independent of Ca^{2+}_i , its smaller effect of increasing the durations of the gaps between bursts approximately threefold was only observed in 0 Ca^{2+}_i (Fig. 2 D). A threefold increase in the durations of the gaps between bursts in 0 Ca^{2+}_i , but not in higher Ca^{2+}_i , would arise if the β_1 subunit selectively slowed $k(n)$, where $n = 0$, threefold, while having little effect on $k(n)$ where $n = 1-4$. If this were the case, Ca^{2+}_i would switch off the lengthening effect of the β_1 subunit on gap duration. Alternatively, the addition of Ca^{2+}_i might remove the lengthening effect of the β_1 subunit by driving the gating away from the altered transition pathways involved in the lengthening, or by selectively changing these pathways. Under conditions of 0 Ca^{2+}_i , the ~ 20 -fold increase in burst duration overrides the smaller threefold increase in gap duration, giving rise to the observed 10-fold increase in P_o with the β_1 subunit in 0 Ca^{2+}_i . In the presence of Ca^{2+}_i , the β_1 subunit no longer lengthens the duration of the gaps between bursts (and may shorten them slightly), so the increase in burst duration can give rise to an even greater increase in P_o , which becomes limited as P_o saturates near its maximum of 0.96.

As indicated above, the β_1 subunit only slows $k(n)$ in the absence of Ca^{2+}_i when $n = 0$. The presence of Ca^{2+}_i switches off the inhibitory effect of the β_1 subunit in 0 Ca^{2+}_i of increasing gap duration. This switching occurs over a range of Ca^{2+}_i between 0.2 and 2 μM (Fig. 2 D). This Ca^{2+} -dependent removal of the inhibition accounted for $\sim 20\%$ of the shift in the apparent Ca^{2+} sensitivity, while the Ca^{2+} -independent increase in burst duration accounted for the other 80% of the shift in apparent Ca^{2+} sensitivity (Fig. 2, A and B).

Conclusion

Ca^{2+}_i is not required for the coupling of the β_1 subunit to the BK channel. In the absence of Ca^{2+}_i , the β_1 subunit increases mean burst duration ~ 20 -fold and also increases the duration of the gaps between bursts approximately threefold. The increase in burst duration facilitates channel activity and the increase in gap duration inhibits channel activity, for an increase in P_o of ~ 10 fold

in 0 Ca^{2+}_i . The β_1 subunit-induced ~ 20 -fold increase in mean burst duration is Ca^{2+} independent, is retained over wide ranges of Ca^{2+}_i and voltage, and accounts for 80% of the increased Ca^{2+} sensitivity associated with the β_1 subunit. The β_1 subunit-induced approximately threefold increase in the duration of gaps between bursts is switched off (inhibited) by the addition of Ca^{2+}_i . This removal of the β_1 subunit-induced inhibition accounts for the remaining 20% of the increased Ca^{2+} sensitivity associated with the β_1 subunit. Thus, the major effect of the β_1 subunit on increasing Ca^{2+} sensitivity occurs through changes in Ca^{2+} -independent rate constants.

We thank Merck Research Laboratories for providing the *mslo* (initially cloned by Pallanck and Ganetzky, 1994) and bovine β_1 clones used for transfection.

This work was supported by a fellowship from the American Heart Association, Florida Affiliate to C.M. Nimigean, and grants from the National Institutes of Health (AR32805) and the Muscular Dystrophy Association to K.L. Magleby.

Submitted: 7 February 2000

Revised: 12 April 2000

Accepted: 13 April 2000

REFERENCES

- Adams, D.J., and P.W. Gage. 1980. Divalent ion currents and the delayed potassium conductance in an *Aplysia* neurone. *J. Physiol.* 304:297–313.
- Adelman, J.P., K.Z. Shen, M.P. Kavanaugh, R.A. Warren, Y.N. Wu, A. Lagrutta, C.T. Bond, and R.A. North. 1992. Calcium-activated potassium channels expressed from cloned complementary DNAs. *Neuron.* 9:209–216.
- Atkinson, N.S., G.A. Robertson, and B. Ganetzky. 1991. A component of calcium-activated potassium channels encoded by the *Drosophila slo* locus. *Science.* 253:551–555.
- Barrett, J.N., K.L. Magleby, and B.S. Pallotta. 1982. Properties of single calcium-activated potassium channels in cultured rat muscle. *J. Physiol.* 331:211–230.
- Blatz, A.L., and K.L. Magleby. 1987. Calcium-activated potassium channels. *TINS (Trends Neurosci.)* 10:463–467.
- Brayden, J.E., and M.T. Nelson. 1992. Regulation of arterial tone by activation of calcium-dependent potassium channels. *Science.* 256:532–535.
- Butler, A., S. Tsunoda, D.P. McCobb, A. Wei, and L. Salkoff. 1993. *mSlo*, a complex mouse gene encoding “maxi” calcium-activated potassium channels. *Science.* 261:221–224.
- Colquhoun, D., and A.G. Hawkes. 1981. On the stochastic properties of single ion channels. *Proc. R. Soc. Lond. B Biol. Sci.* 211:205–235.
- Colquhoun, D., and A.G. Hawkes. 1982. On the stochastic properties of bursts of single ion channel openings and of clusters of bursts. *Philos. Trans. R. Soc. Lond. B Biol. Sci.* 300:1–59.
- Colquhoun, D., and A.G. Hawkes. 1995. The principles of the stochastic interpretation of ion channel mechanisms. In *Single-Channel Recording*. B. Sakmann and E. Neher, editors. Plenum Publishing Corp., New York, NY. 397–482.
- Colquhoun, D., and F.J. Sigworth. 1995. Fitting and statistical analysis of single-channel records. In *Single-Channel Recording*. B. Sakmann and E. Neher, editors. Plenum Publishing Corp., New York, NY. 483–587.
- Conley, E.C. 1996. *The Ion Channel Facts Book II*. Academic Press, Harcourt Brace & Co., San Diego, CA. 607–720.
- Cook, D.L. 1984. Electrical pacemaker mechanisms of pancreatic islet cells. *Fed. Proc.* 43:2368–2372.
- Cox, D.H., J. Cui, and R.W. Aldrich. 1997. Allosteric gating of a large conductance Ca-activated K^+ channel. *J. Gen. Physiol.* 110:257–281.
- Cox, D.H., and R.W. Aldrich. 2000. Is the BK_{Ca} channel's Ca^{2+} binding affinity enhanced by its β_1 subunit? A simple experiment. *Bio-phys. J.* 78:91A. (Abstr.)
- Cui, J., D.H. Cox, and R.W. Aldrich. 1997. Intrinsic voltage dependence and Ca^{2+} regulation of *mslo* large conductance Ca-activated K^+ channels. *J. Gen. Physiol.* 109:647–673.
- Diaz, L., P. Meera, J. Amigo, E. Stefani, O. Alvarez, L. Toro, and R. Latorre. 1998. Role of the S4 segment in a voltage-dependent calcium-sensitive potassium (*hSlo*) channel. *J. Biol. Chem.* 273:32430–32436.
- DiChiara, T.J., and P.H. Reinhart. 1995. Distinct effects of Ca^{2+} and voltage on the activation and deactivation of cloned Ca^{2+} -activated K^+ channels. *J. Physiol.* 489:403–418.
- Dworetzky, S.I., C.G. Boissard, J.T. Lum-Ragan, M.C. McKay, D.J. Post-Munson, J.T. Trojnecki, C.P. Chang, and V.K. Gribkoff. 1996. Phenotypic alteration of a human BK (*hSlo*) channel by *hSlo* β subunit coexpression: changes in blocker sensitivity, activation/relaxation and inactivation kinetics, and protein kinase A modulation. *J. Neurosci.* 16:4543–4550.
- Dworetzky, S.I., J.T. Trojnecki, and V.K. Gribkoff. 1994. Cloning and expression of a human large-conductance calcium-activated potassium channel. *Brain Res. Mol. Brain Res.* 27:189–193.
- Hamill, O.P., A. Marty, E. Neher, B. Sakmann, and F.J. Sigworth. 1981. Improved patch-clamp techniques for high-resolution current recording from cells and cell-free membrane patches. *Pflügers Arch.* 391:85–100.
- Hille, B. 1991. *Ionic channels of excitable membranes*. Sinauer Associates, Inc., Sunderland, MA. 607 pp.
- Horrigan, F.T., J. Cui, and R.W. Aldrich. 1999. Allosteric voltage gating of potassium channels. I: *mSlo* ionic currents in the absence of Ca^{2+} . *J. Gen. Physiol.* 114:277–305.
- Horrigan, F.T., and R.W. Aldrich. 1999. Allosteric voltage gating of potassium channels. II: *mSlo* channel gating charge movement in the absence of Ca^{2+} . *J. Gen. Physiol.* 114:305–337.
- Hudspeth, A.J., and R.S. Lewis. 1988. A model for electrical resonance and frequency tuning in saccular hair cells of the bullfrog, *Rana catesbeiana*. *J. Physiol.* 400:275–297.
- Jan, L.Y., and Y.N. Jan. 1997. Cloned potassium channels from eukaryotes and prokaryotes. *Annu. Rev. Neurosci.* 20:91–123.
- Jones, E.M., M. Gray-Keller, and R. Fettplice. 1999. The role of Ca^{2+} -activated K^+ channel spliced variants in the tonotopic organization of the turtle cochlea. *J. Physiol.* 518:653–665.
- Kaczorowski, G.J., H.G. Knaus, R.J. Leonard, O.B. McManus, and M.L. Garcia. 1996. High-conductance calcium-activated potassium channels; structure, pharmacology, and function. *J. Bioenerg. Biomembr.* 28:255–267.
- Knaus, H.G., K. Folander, M. Garcia-Calvo, M.L. Garcia, G.J. Kaczorowski, M. Smith, and R. Swanson. 1994. Primary sequence and immunological characterization of β -subunit of high conductance Ca^{2+} -activated K^+ channel from smooth muscle. *J. Biol. Chem.* 269:17274–17278.
- Magleby, K.L. 1992. Ion channels. Preventing artifacts and reducing errors in single-channel analysis. *Methods Enzymol.* 207:763–791.
- Magleby, K.L., and B.S. Pallotta. 1983. Burst kinetics of single calcium-activated potassium channels in cultured rat muscle. *J. Physiol.* 344:605–623.
- Martell, A.E., and R.M. Smith. 1993. NIST Standard Reference Database 46.
- Marty, A. 1981. Ca-dependent K channels with large unitary con-

- ductance in chromaffin cell membranes. *Nature*. 291:497–500.
- Marty, A. 1983. Ca-dependent potassium channels with large unitary conductance. *Trends Neurosci*. 6:262–265.
- Maruyama, Y., O.H. Petersen, P. Flanagan, and G.T. Pearson. 1983. Quantification of Ca²⁺-activated K⁺ channels under hormonal control in pig pancreas acinar cells. *Nature*. 305:228–232.
- McManus, O.B., A.L. Blatz, and K.L. Magleby. 1987. Sampling, log binning, fitting, and plotting durations of open and shut intervals from single channels and the effects of noise. *Pflügers Arch*. 410:530–553.
- McManus, O.B., and K.L. Magleby. 1988. Kinetic states and modes of single large-conductance calcium-activated potassium channels in cultured rat skeletal muscle. *J. Physiol*. 402:79–120.
- McManus, O.B., and K.L. Magleby. 1989. Kinetic time constants independent of previous single-channel activity suggest Markov gating for a large conductance Ca-activated K channel. *J. Gen. Physiol*. 94:1037–1070.
- McManus, O.B., and K.L. Magleby. 1991. Accounting for the Ca²⁺-dependent kinetics of single large-conductance Ca²⁺-activated K⁺ channels in rat skeletal muscle. *J. Physiol*. 443:739–777.
- McManus, O.B., L.M. Helms, L. Pallanck, B. Ganetzky, R. Swanson, and R.J. Leonard. 1995. Functional role of the β subunit of high conductance calcium-activated potassium channels. *Neuron*. 14:645–650.
- Meech, R.W., and N.B. Standen. 1975. Potassium activation in *Helix aspersa* neurones under voltage clamp: a component mediated by calcium influx. *J. Physiol*. 249:211–259.
- Meech, R.W. 1978. Calcium-dependent potassium activation in nervous tissues. *Annu. Rev. Biophys. Bioeng*. 7:1–18.
- Meera, P., M. Wallner, Z. Jiang, and L. Toro. 1996. A calcium switch for the functional coupling between α (*hsl α*) and β subunits (K_{vCa}) of maxi K channels. *FEBS Lett*. 382:84–88.
- Meera, P., M. Wallner, M. Song, and L. Toro. 1997. Large conductance voltage- and calcium-dependent K⁺ channel, a distinct member of voltage-dependent ion channels with seven N-terminal transmembrane segments (S0–S6), an extracellular N terminus, and an intracellular (S9–S10) C terminus. *Proc. Natl. Acad. Sci. USA*. 94:14066–14071.
- Monod, J., J. Wyman, and J.-P. Changeux. 1965. On the nature of allosteric transitions: a plausible model. *J. Mol. Biol*. 12:88–118.
- Nimigeon, C.M., and K.L. Magleby. 1999. The β subunit increases the Ca²⁺ sensitivity of large conductance Ca²⁺-activated potassium channels by retaining the gating in the bursting states. *J. Gen. Physiol*. 113:425–439.
- Oberst, C., R. Weiskirchen, M. Hartl, and K. Bister. 1997. Suppression in transformed avian fibroblasts of a gene (CO6) encoding a membrane protein related to mammalian potassium channel regulatory subunits. *Oncogene*. 14:1109–1116.
- Pallanck, L., and B. Ganetzky. 1994. Cloning and characterization of human and mouse homologs of the *Drosophila* calcium-activated potassium channel gene, *slowpoke*. *Hum. Mol. Genet*. 3:1239–1243.
- Pallotta, B.S., K.L. Magleby, and J.N. Barrett. 1981. Single channel recordings of Ca²⁺-activated K⁺ currents in rat muscle cell culture. *Nature*. 293:471–474.
- Pallotta, B.S. 1985. *N*-Bromoacetamide removes a calcium-dependent component of channel opening from calcium-activated potassium channels in rat skeletal muscle. *J. Gen. Physiol*. 86:601–611.
- Petersen, O.H., and I. Findlay. 1987. Electrophysiology of the pancreas. *Physiol. Rev*. 67:1054–1116.
- Ramanathan, K., T.H. Michael, and P.A. Fuchs. 2000. β_1 subunits modulate alternatively spliced, large conductance, calcium-activated potassium channels of avian hair cells. *J. Neurosci*. 20:1675–1684.
- Rothberg, B.S., R.A. Bello, L. Song, and K.L. Magleby. 1996. High Ca²⁺ concentrations induce a low activity mode and reveal Ca²⁺-independent long shut intervals in BK channels from rat muscle. *J. Physiol*. 493:673–689.
- Rothberg, B.S., and K.L. Magleby. 1998. Kinetic structure of large-conductance Ca²⁺-activated K⁺ channels suggests that the gating includes transitions through intermediate or secondary states. A mechanism for flickers. *J. Gen. Physiol*. 111:751–780.
- Rothberg, B.S., and K.L. Magleby. 1999. Gating kinetics of single large-conductance Ca²⁺-activated K⁺ channels in high Ca²⁺ suggest a two-tiered allosteric gating mechanism. *J. Gen. Physiol*. 114:93–124.
- Salkoff, L., K. Baker, A. Butler, M. Covarrubias, M.D. Pak, and A. Wei. 1992. An essential 'set' of K⁺ channels conserved in flies, mice and humans. *TINS (Trends Neurosci)*. 15:161–166.
- Schreiber, M., and L. Salkoff. 1997. A novel calcium-sensing domain in the BK channel. *Biophys. J*. 73:1355–1363.
- Schreiber, M., A. Yuan, and L. Salkoff. 1999. Transplantable sites confer calcium sensitivity to BK channels. *Nat. Neurosci*. 2:416–421.
- Sigworth, F.J., and S.M. Sine. 1987. Data transformations for improved display and fitting of single-channel dwell time histograms. *Biophys. J*. 52:1047–1054.
- Singer, J.J., and J.V. Walsh, Jr. 1987. Characterization of calcium-activated potassium channels in single smooth muscle cells using the patch-clamp technique. *Pflügers Arch*. 408:98–111.
- Smart, T.G. 1987. Single calcium-activated potassium channels recorded from cultured rat sympathetic neurones. *J. Physiol*. 389:337–360.
- Smith, G.L., and D.J. Miller. 1985. Potentiometric measurements of stoichiometric and apparent affinity constants of EGTA for protons and divalent ions including calcium. *Biochim. Biophys. Acta*. 839:287–299.
- Stefani, E., M. Ottolia, F. Noceti, R. Olcese, M. Wallner, R. Latorre, and L. Toro. 1997. Voltage-controlled gating in a large conductance Ca²⁺-sensitive K⁺ channel (*hsl α*). *Proc. Natl. Acad. Sci. USA*. 94:5427–5431.
- Tanaka, Y., P. Meera, M. Song, H.-G. Knaus, and L. Toro. 1997. Molecular constituents of maxi K_{Ca} channels in human coronary smooth muscle: predominant $\alpha + \beta$ subunit complexes. *J. Physiol*. 502:545–557.
- Talukder, G., and R.W. Aldrich. 2000. Complex voltage-dependent behavior of single unliganded calcium-sensitive potassium channels. *Biophys. J*. 78:761–772.
- Tseng-Crank, J., C.D. Foster, J.D. Krause, R. Mertz, N. Godinot, T.J. DiChiara, and P.H. Reinhart. 1994. Cloning, expression, and distribution of functionally distinct Ca²⁺-activated K⁺ channel isoforms from human brain. *Neuron*. 13:1315–1330.
- Tseng-Crank, J., N. Godinot, T.E. Johansen, P.K. Ahring, D. Strobaek, R. Mertz, C.D. Foster, S.P. Olesen, and P.H. Reinhart. 1996. Cloning, expression, and distribution of a Ca²⁺-activated K⁺ channel β -subunit from human brain. *Proc. Natl. Acad. Sci. USA*. 93:9200–9205.
- Wallner, M., P. Meera, M. Ottolia, G.J. Kaczorowski, R. Latorre, M.L. Garcia, E. Stefani, and L. Toro. 1995. Characterization of and modulation by a β -subunit of a human maxi K_{Ca} channel cloned from myometrium. *Receptors Channels*. 3:185–199.
- Wallner, M., P. Meera, and L. Toro. 1996. Determinant for β -subunit regulation in high-conductance voltage-activated and Ca²⁺-sensitive K⁺ channels: an additional transmembrane region at the N terminus. *Proc. Natl. Acad. Sci. USA*. 93:14922–14927.
- Wallner, M., P. Meera, and L. Toro. 1999. Molecular basis of fast inactivation in voltage and Ca²⁺-activated K⁺ channels: a transmembrane β -subunit homolog. *Proc. Natl. Acad. Sci. USA*. 96:4137–4142.
- Wei, A., C. Solaro, C. Lingle, and L. Salkoff. 1994. Calcium sensitivity of BK-type K_{Ca} channels determined by a separable domain. *Neuron*. 13:671–681.
- Wu, Y.C., J.J. Art, M.B. Goodman, and R. Fettiplace. 1995. A kinetic description of the calcium-activated potassium channel and its application to electrical tuning of hair cells. *Prog. Biophys. Mol. Biol*. 63:131–158.
- Xia, X.M., J.P. Ding, and C.J. Lingle. 1999. Molecular basis for the inactivation of Ca²⁺- and voltage-dependent BK channels in adrenal chromaffin cells and rat insulinoma tumor cells. *J. Neurosci*. 19:5255–5264.